Antenna Doping: The Key for Achieving Efficient Optical Wavelength Conversion in Crystalline Chromophoric Heterolayers

Ritesh Haldar, Hongye Chen, Antoine Mazel, Dong-Hui Chen, Gaurav Gupta, Navneet Dua, Stephane Diring, Fabrice Odobel, Christof Wöll

HAL Id: hal-03384232

Antenna Doping: The Key for Achieving Efficient Optical Wavelength Conversion in Crystalline Chromophoric Heterolayers

Ritesh Haldar,*[a‡] Hongye Chen,[ab‡] Antoine Mazel,[c] Dong-Hui Chen,[a] Gaurav Gupta,[a] Navneet Dua,[a] Stéphane Diring,*[c] Fabrice Odobel,*[c] and Christof Wöll*[a]

[a]Karlsruhe Institute of Technology (KIT), Institute of Functional Interfaces (IFG), Hermann-von-Helmholtz Platz-1, 76344 Eggenstein-Leopoldshafen (Germany).
E-mail: ritesh.haldar@kit.edu; christof.woell@kit.edu

[b]State Key Laboratory of Mechanics and Control of Mechanical Structures, Key Laboratory for Intelligent Nano Materials and Devices of the MOE, Institute of Nano Science, Nanjing University of Aeronautics and Astronautics, Nanjing, 210016, China.

[c]Université de Nantes, CNRS, CEISAM UMR 6230, F-44000, Nantes, France.
E-mail: stephane.diring@univ-nantes.fr; fabrice.odobel@univ-nantes.fr

‡ These authors contributed equally.

Abstract: High-yield wavelength conversion is one of the key requirements for efficient photon energy harvesting. Attempts to realize efficient conversion by simply stacking layers of chromophores have failed so far, even when using highly crystalline assemblies and employing the recently discovered long-range (>100 nm) Förster resonance energy transfer, LR-FRET. We were able to drastically improve optical conversion efficiency by using chromophoric metal-organic framework (MOF) heterolayers fabricated using layer-by-layer techniques in connection with an "antenna doping" strategy. Systematic investigations revealed that the LR-FRET mechanism, reported previously in chromophoric aggregates, is highly anisotropic for neat materials but can be made more isotropic by employing doping strategies. Using optimized fabrication parameters and dopant concentrations, a three-layer, two-step cascade with an overall optical conversion efficiency of ~ 75% has been realized.

Introduction

Photon absorption and subsequent transport of the resulting excitations are key steps in the conversion of light to other forms of energy. For efficient light absorption, a huge variety of dyes is available, both from nature[1] as well as from organic synthesis, many of them relying on extended π-conjugated structures.[2-3] To avoid reemission, the energy stored in form of electronic excitations must be transported to regions in space where they are converted into another form of energy, either chemical or electrical. In mesoscale assemblies, this exciton transport is often inefficient since abundant unwanted inter-chromophore interactions lead to non-radiative deactivation or fluorescence quenching. Some of the commonly encountered loss processes result from H-type aggregate formation, structural defects, unwanted electron transfer (charge separation), etc.[4-6] In order to avoid such losses upon energy transfer, high purity, structurally perfect structures are required. Furthermore, established device architectures require a directional transport of excitons, isotropic processes will greatly reduce device performance. [7]

The most efficient transfer mechanism for singlet excitons is Förster resonance energy transfer (FRET). This mechanism allows to realize a wavelength converter together with directional energy transport in a straightforward fashion by arranging suitable donor-acceptor (D-A) pairs into a chain, e.g. consisting of three different chromophores C1, C2, and C3, as illustrated in Figure 1a. If the emission of C1 and the absorption of C2, as well as the emission of C2 and the absorption of C3 show sufficient spectral overlap, efficient FRET will cause the trimer to function as a two-step cascade, i.e. causing directed energy conversion of photons absorbed in C1 via C2 to C3 (Figure 1a-b).

On the molecular level, a variety of organic synthesis schemes for the fabrication of such cascades have been reported, most of them based on sophisticated coupling chemistry using suitable building blocks.[8] However, for integration into organic photovoltaic (OPV) devices, mesoscopic assemblies providing transport on a macroscopic scale are mandatory.[9] While a number of approaches have been presented to fabricate such chromophoric aggregates, e.g. based on zeolites,[10] solvated molecules, or gels (randomly oriented), as well as dendritic systems,[11-14] only few of these strategies are compatible with contemporary OPV device architectures. Moreover, most of these previously reported aggregates are limited by a fairly large number of structural imperfections, which lead to quenching of excitons.

An emerging strategy to yield chromophoric aggregates is based on MOFs, a large class of crystalline network materials, originally introduced for applications in gas storage

and separation.[15-18] These porous coordination polymers have more recently found new applications in optoelectronics, including light harvesting, photo-conductivity, non-linear optics, etc.[19-27] In particular, metal-organic framework thin films, SURMOFs, built from chromophoric linkers using layer-by-layer methods, have been shown to allow for the construction of photoactive aggregates with well-defined photophysical properties and low densities of defects. Such high optical quality MOF thin films were successfully used for photon upconversion, highly anisotropic, directional transport of excitons, J-aggregate formation,[28] and as active medium in optical cavities.[29]
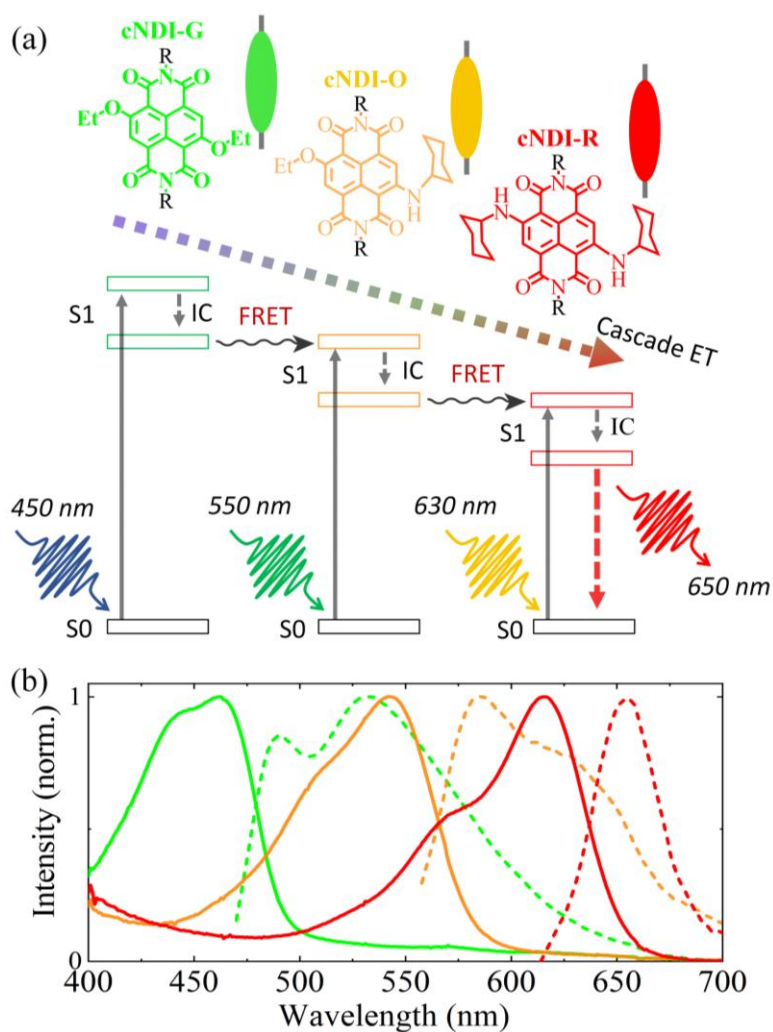
Figure 1. (a) Schematic of a cascade FRET among cNDI-G, -O and -R and chemical structures of the linkers; R group attached to the imide-N is a 3,5-diisopropylbenzoic acid (see supporting information); (b) Absorbance (solid) and fluorescence (dotted) spectra of Zn-cNDI-G, -O, and -R SURMOFs. All of the spectra are recorded at room temperature.

Considering the requirements listed above for fabricating energy conversion cascades, it seems straightforward, following the scheme depicted in Fig. 1, to realize trilayer systems of chromophoric SURMOFs, exploiting the fact that the layer-by-layer methods are well suited to fabricate hetero-multilayer.[30] A particular advantage of chromophoric SURMOFs is the crystallinity and high degree or orientation of these thin films, resulting in very high absorption efficiency[31] and the emergence of long-range anisotropic FRET transfer.[32-33]

Results and discussion

The approach presented here is based on three complementary core-substituted naphthalenediimide based linkers (cNDIs),[34] bis- ethoxy- naphthalenediimide (cNDI-G), ethoxy-cyclohexylamine-naphthalenediimide (cNDI-O) and bis-cyclohexylamine-naphthalenediimide (cNDI-R) (Figure 1a). The absorption and emission profiles of these three dyes in the SURMOF structure show the spectral overlap of emission and absorption bands required for the realization of a two-step energy converter (Figure 1b and Figure S1). The individual steps are a FRET process from the blue light absorbing bottom cNDI-G layer first to a center cNDI-O, and from there to a top layer of cNDI-R, from where the energy is emitted as red light. The individual chromophoric linkers were chosen such that within a single MOF layer they form J-aggregates (as reported previously),[6, 35] an arrangement which is highly beneficial for yielding strong absorption and high fluorescence quantum yields. The stacked trilayer SURMOF system was deposited on hydroxyl- terminated surfaces using a lbl spin-coating fabrication method as described previously.[35-36]

The basic MOF type used for the present study is Zn-SURMOF-2.[37-38] The key structural element of this reticular materials are ditopic dicarboxylate linkers, which are connected to Zn^{++} ions yielding so-called paddle-wheel units. These secondary building units (SBUs) then form 2D square-grid-like structures exhibiting a *P*4 symmetry (Figure 2a). Using the liquid-phase epitaxy method with optimized parameters in connection with hydroxyl terminated surfaces, we fabricated structurally well-defined Zn-SURMOF-2 thin films with [001] orientation, as shown in Figure 2a. The structure was the same for all three different chromophoric linkers (see experimental section in the Supporting Information). The X-ray diffraction (XRD) data revealed that the three SURMOFs were isostructural (Figure 2b), with the cNDI-based linkers stacked along the [010] crystallographic direction (oriented parallel to

the substrate), with an inter-linker distance of 6.8 Å.[35]. We thus conclude that the modification of the core substitution group in the NDI-linkers did not alter the unit cell parameters of these chromophoric crystalline structures,[36] a key requirement for achieving good heteroepitaxial growth.
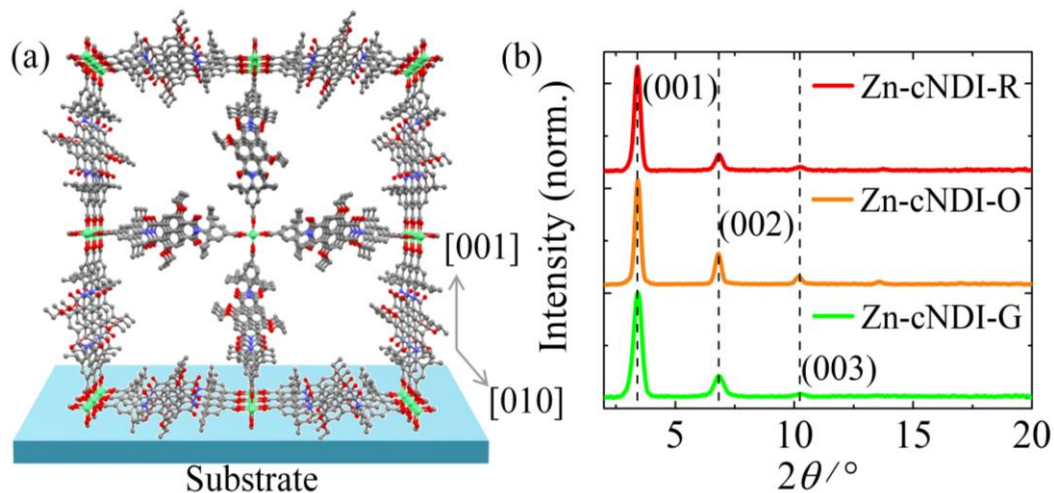
Figure 2. (a) Zn-cNDI-G structure epitaxially grown along (001) direction; (b) Out-of-plane XRD patterns of three Zn-SURMOF-2 films (green for Zn-cNDI-G, orange for Zn-cNDI-O and red for Zn-cNDI-R).

The 2D packing of the c-NDI chromophores results in the formation of J-aggregates[35] with excellent lateral (intra-layer) coupling. As a result of this pronounced structural anisotropy, Förster energy transport is very efficient parallel to the substrate,[39] but very poor (lower by a factor of 1000) perpendicular to the layers. The energy transfer perpendicular to the substrate is thus severely limited. This fact, which is a main obstacle for the realization of a conversion cascade, is demonstrated by the data shown in Figure S2a-b. Excitation of a bilayer heterostructure of Zn-cNDI-G/Zn-cNDI-O (HL-1) at450 nm resulted in two emission bands, one at 530 nm from the bottom layer and one at 580 nm from the top layer. The presence of the 530 nm emission band from Zn-cNDI-G reveals that the energy transfer is inefficient – clearly a substantial fraction of the absorbed energy is not transferred to the top layer but reemitted from the bottom SURMOF. In fact, the small amount of emission at 580 nm is not due to a small amount of energy transfer across the interface, but due to direct absorption of the 450 nm excitation light. This was demonstrated by the following experiment. We fabricated a test structure with an additional separator layer (~80 nm FRET inactive layer) between Zn-cNDI-G and Zn-cNDI-O (see Figure 3S2a (HL-1-sep, Figure S3). Since the separator should efficiently prohibit any FRET energy transfer, the fact that

emission at ~580 nm could still be observed unequivocally demonstrates that this emission results from direct excitation (Figure S2b) – and not from FRET transfer.

This observation makes clear that the main obstacle to realizing the conversion cascade is the poor inter-layer energy transfer. Although in the previous work long-range FRET has been reported in such aggregated chromophoric systems,[32-33] our results suggest that this transfer must be highly anisotropic. Obviously, the excellent, crystalline order makes the energy transfer so anisotropic that inter-layer coupling becomes impossible.

At this point we speculated that the intentional introduction of defects allowing for a more isotropic coupling might be beneficial. Of course, such doping must avoid the introduction of structural defects, since they could lead to unwanted quenching effects.[40] Therefore, we introduced dopants in form of different MOF linkers with the same length. The resulting structure with "antennas" introduced into SURMOFs is shown in Figure 3a. The bottom Zn-cNDI-G layer was doped with acceptor cNDI-O linkers and the top Zn-cNDI-O layer with cNDI-R. Indeed, Fig. 3b shows that this strategy was successful; the HL-2 SURMOF exhibited only red emission at 630 nm upon excitation at 450 nm. The absence of any emission at 530 and 580 nm revealed that now all the energy absorbed in the bottom layer is efficiently transferred to the upper cNDI-R layer, a two-step conversion cascade has been realized successfully.

The optimization of the antenna doping levels (i.e. the concentration of the emitter chromophores within the individual J-aggregate SURMOFs) to achieve maximum intra-layer energy transfer was carried out as following. First, the energy acceptor (emitter) cNDI concentration in the donor layer was enhanced until the donor emission was almost quenched, i.e. a maximum energy transfer to the next layer is achieved. Figure S4 and S5 show the concentration dependent emission spectra of those mixed-cNDI SURMOFs (Figure S6). We observed a maximum of ~ 90 and 85% energy transfer efficiency, in cNDI-O doped Zn-cNDI-G and cNDI-R doped Zn-cNDI-O layer, respectively, as estimated from a comparison of the donor and acceptor emission intensities. The high efficiency within the layer is expected, because of strong intra-cNDI J-coupling. Based on these experiments we chose 1.6% cNDI-O/Zn-cNDI-G as bottom layer (thickness ~ 20 nm), 1.9% cNDI-R/Zn-cNDI-O as middle layer (thickness ~ 20 nm), and top layer of Zn-cNDI-R to construct a trilayer film HL-2 (Figure 3 and Figure S7a). Excitation of HL-2 at 450 nm exhibited absence of emission corresponding to the bottom layer Zn-cNDI-G, and intense emission from Zn-cNDI-R,

demonstrating a high efficiency[41-42] (~ 75%) cross-layer energy transfer to the top acceptor layer (Figure 3b and S7b). In the absence of the antenna dopants, a trilayer HL-3 (i.e. Zn-cNDI-G/Zn-cNDI-O/Zn-cNDI-R, 20 nm each layer) showed no red emission, indicating absence of intralayer-FRET (Figure 3b, gray line).

The observed efficient energy transfer is also supported by the following experiments; (i) the excitation spectrum monitored at 640 nm (i.e. top layer, cNDI-R emission) showed a maximum corresponding to Zn-cNDI-G and Zn-cNDI-O which is indicating that bottom layer energy is being transported to the top acceptor layer (Figure S8); (ii) strong fluorescence intensity observed by 450 nm excitation compared to that by 580 nm excitation (Figure S9); (iii) a strong reduction of fluorescence lifetime at 500 nm reconfirmed the energy transfer (Figure S10). The fluorescence quantum yield of HL-2 was found to be ~ 10.5±1 %, which is higher than pristine Zn-cNDI-G (~2.3±0.5 %),[35] and Zn-cNDI-R (~2.9±0.4%) indicating efficient energy harvesting in a cascade process.

We rationalize the findings reported above by proposing that the antennas invoke LR-FRET also perpendicular to the layers. To confirm this hypothesis, and to determine the range of this transfer-process, we have constructed a second set of model heterostructures (c-HL), similar to that described above. In this case, instead of neat chromophoric SURMOFs, doped MOF thin layers were used (see Fig. S11a, passive layer marked in gray). Fig S11b demonstrates that the emission from the top-layer at 650 nm is intense in the absence of a separator (red), but weak for large separations (20 nm, black) (Fig. S10b). As expected for LR-FRET [43], [32-33] the energy transfer occurs over rather long distances of >10 nm, far longer than in normal FRET processes.
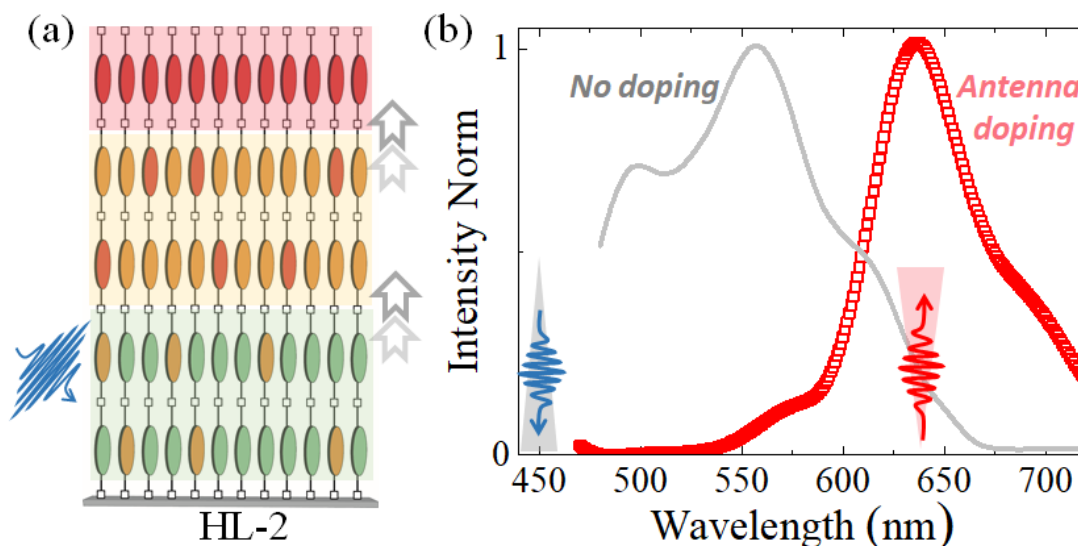
Figure 3. (a) Schematic of the HL-2 heterostructure with antenna doping design, (b) emission spectrum of the HL-2 and a non-doped trilayer structure (HL-3), recorded upon excitation at 450 nm at room temperature.

Conclusions

In conclusion, we have demonstrated a two-step cascade for wavelength conversion by assembling three different cNDI chromophores into heterolayer monolithic MOF thin films. Blue light was efficiently harvested and converted to red light across the SURMOF interface. To achieve high-yield, cross-layer FRET, we have developed an "antenna doping" strategy. Introducing isolated FRET emitters within the anisotropic J-aggregates allowed us to overcome the strong directionality of the previously observed LR-FRET mechanism and to achieve efficient inter-layer energy transfer. By optimization of the doping concentrations in the heterolayers, we could achieve (i) ~75% energy conversion and (ii) fluorescence quantum yield enhancement of ~4-times compared to pristine individual SURMOFs. This new design strategy based on a layer-by-layer heteroepitaxy process in combination with doping strategies opens up new numerous options for optoelectronic device architectures.

References:

1.   Scholes, G. D., Fleming, G. R., Olaya-Castro, A. & Van Grondelle, R., Lessons from nature about solar light harvesting, *Nature Chemistry*, **3**, 763 (2011).

2.   Wu, S.-L., et al., Design and characterization of porphyrin sensitizers with a push-pull framework for highly efficient dye-sensitized solar cells, *Energy & Environmental Science*, **3**, 949-955 (2010).

3.   Lu, J., Liu, S. & Wang, M., Push-Pull Zinc Porphyrins as Light-Harvesters for Efficient Dye-Sensitized Solar Cells, *Frontiers in Chemistry*, **6** (2018).

4.   Singh, D. K., Iyer, P. K. & Giri, P. K., Role of molecular interactions and structural defects in the efficient fluorescence quenching by carbon nanotubes, *Carbon*, **50**, 4495-4505 (2012).

5.   Doose, S., Neuweiler, H. & Sauer, M., Fluorescence Quenching by Photoinduced Electron Transfer: A Reporter for Conformational Dynamics of Macromolecules, *ChemPhysChem*, **10**, 1389-1398 (2009).

6.   Würthner, F., Kaiser, T. E. & Saha-Möller, C. R., J-Aggregates: From Serendipitous Discovery to Supramolecular Engineering of Functional Dye Materials, *Angewandte Chemie International Edition*, **50**, 3376-3410 (2011).

7.   Azzouzi, M., et al., Nonradiative Energy Losses in Bulk-Heterojunction Organic Photovoltaics, *Physical Review X*, **8**, 031055 (2018).

8.   Tsubaki, K., et al., Three-component cascade energy transfer with use of oligonaphthalene skeletons, *The Journal of organic chemistry*, **73**, 4279-4282 (2008).

9.   Lu, L., et al., Recent Advances in Bulk Heterojunction Polymer Solar Cells, *Chemical Reviews*, **115**, 12666-12731 (2015).

10.   Calzaferri, G., Huber, S., Maas, H. & Minkowski, C., Host–guest antenna materials, *Angewandte Chemie International Edition*, **42**, 3732-3758 (2003).

11.   Serin, J. M., Brousmiche, D. W. & Fréchet, J. M., Cascade energy transfer in a conformationally mobile multichromophoric dendrimer, *Chemical Communications*, 2605-2607 (2002).

12.   Balzani, V., et al., Dendrimers based on photoactive metal complexes. Recent advances, *Coordination Chemistry Reviews*, **219**, 545-572 (2001).

13.   Diring, S., Puntoriero, F., Nastasi, F., Campagna, S. & Ziessel, R., Star-shaped multichromophoric arrays from bodipy dyes grafted on truxene core, *Journal of the American Chemical Society*, **131**, 6108-6110 (2009).

14.   Rao, K. V., Datta, K. K. R., Eswaramoorthy, M. & George, S. J., Light-Harvesting Hybrid Assemblies, *Chemistry – A European Journal*, **18**, 2184-2194 (2012).

15.   Furukawa, H., Cordova, K. E., O'Keeffe, M. & Yaghi, O. M., The Chemistry and Applications of Metal-Organic Frameworks, *Science*, **341**, 1230444 (2013).

16.   Kitagawa, S., Kitaura, R. & Noro, S. i., Functional porous coordination polymers, *Angewandte Chemie International Edition*, **43**, 2334-2375 (2004).

17.   Suh, M. P., Park, H. J., Prasad, T. K. & Lim, D.-W., Hydrogen Storage in Metal–Organic Frameworks, *Chemical Reviews*, **112**, 782-835 (2012).

18.   Li, J.-R., Sculley, J. & Zhou, H.-C., Metal–Organic Frameworks for Separations, *Chemical Reviews*, **112**, 869-932 (2012).

19.   Hu, Z., Deibert, B. J. & Li, J., Luminescent metal–organic frameworks for chemical sensing and explosive detection, *Chemical Society Reviews*, **43**, 5815-5840 (2014).

20.   D'Alessandro, D. M., Exploiting redox activity in metal–organic frameworks: concepts, trends and perspectives, *Chemical Communications*, **52**, 8957-8971 (2016).

21.   Stavila, V., Talin, A. & Allendorf, M., MOF-based electronic and opto-electronic devices, *Chemical Society Reviews*, **43**, 5994-6010 (2014).

22.   Liu, J., et al., Photoinduced Charge-Carrier Generation in Epitaxial MOF Thin Films: High Efficiency as a Result of an Indirect Electronic Band Gap?, *Angewandte Chemie International Edition*, **54**, 7441-7445 (2015).

23.   Zhang, T. & Lin, W., Metal–organic frameworks for artificial photosynthesis and photocatalysis, *Chemical Society Reviews*, **43**, 5982-5993 (2014).

24.   Lee, C. Y., et al., Light-Harvesting Metal–Organic Frameworks (MOFs): Efficient Strut-to-Strut Energy Transfer in Bodipy and Porphyrin-Based MOFs, *Journal of the American Chemical Society*, **133**, 15858-15861 (2011).

25.   Liu, X., et al., Photoconductivity in Metal–Organic Framework (MOF) Thin Films, *Angewandte Chemie International Edition*, **58**, 9590-9595 (2019).

26. Medishetty, R., Zaręba, J. K., Mayer, D., Samoć, M. & Fischer, R. A., Nonlinear optical properties, upconversion and lasing in metal–organic frameworks, *Chemical Society Reviews*, **46**, 4976-5004 (2017).

27. Stassen, I., et al., An updated roadmap for the integration of metal–organic frameworks with electronic devices and chemical sensors, *Chemical Society Reviews*, **46**, 3185-3241 (2017).

28. Haldar, R., Heinke, L. & Wöll, C., Advanced Photoresponsive Materials Using the Metal–Organic Framework Approach, *Advanced Materials*, **32**, 1905227 (2020).

29. Haldar, R., et al., Guest-responsive polaritons in a porous framework: chromophoric sponges in optical QED cavities, *Chemical Science*, **11**, 7972-7978 (2020).

30. Haldar, R. & Wöll, C., Hierarchical assemblies of molecular frameworks—MOF-on-MOF epitaxial heterostructures, *Nano Research* (2020).

31. Jia, J., et al., Access to Highly Efficient Energy Transfer in Metal–Organic Frameworks via Mixed Linkers Approach, *J.Am. Chem. Soc*, **142**, 8580-8584 (2020).

32. Zhang, Q., et al., Förster Energy Transport in Metal–Organic Frameworks Is Beyond Step-by-Step Hopping, *J.Am. Chem. Soc*, **138**, 5308-5315 (2016).

33. Shaikh, Shaunak M., et al., Light harvesting and energy transfer in a porphyrin-based metal organic framework, *Faraday Discussions*, **216**, 174-190 (2019).

34. Sakai, N., Mareda, J., Vauthey, E. & Matile, S., Core-substituted naphthalenediimides, *Chemical Communications*, **46**, 4225-4237 (2010).

35. Haldar, R., et al., A de novo strategy for predictive crystal engineering to tune excitonic coupling, *Nature Communications*, **10**, 2048 (2019).

36. Haldar, R., et al., Excitonically Coupled States in Crystalline Coordination Networks, *Chemistry A European Journal*, **23**, 14316-14322 (2017).

37. Liu, J., et al., A novel series of isoreticular metal organic frameworks: realizing metastable structures by liquid phase epitaxy, *Scientific Reports*, **2**, 921 (2012).

38. Haldar, R., et al., Enhancing Selectivity and Kinetics in Oxidative Photocyclization by Supramolecular Control, *Angewandte Chemie International Edition*, **57**, 13662-13665 (2018).

39. Haldar, R., et al., Anisotropic energy transfer in crystalline chromophore assemblies, *Nature Communications*, **9**, 4332 (2018).

40. Schrimpf, W., et al., Chemical diversity in a metal–organic framework revealed by fluorescence lifetime imaging, *Nature Communications*, **9**, 1647 (2018).

41. So, M. C., et al., Layer-by-Layer Fabrication of Oriented Porous Thin Films Based on Porphyrin-Containing Metal–Organic Frameworks, *Journal of the American Chemical Society*, **135**, 15698-15701 (2013).

42. Park, H. J., et al., Layer-by-Layer Assembled Films of Perylene Diimide- and Squaraine-Containing Metal–Organic Framework-like Materials: Solar Energy Capture and Directional Energy Transfer, *ACS Applied Materials & Interfaces*, **8**, 24983-24988 (2016).

43. Bell, T. D. M., et al., Synthesis and Photophysics of Core-Substituted Naphthalene Diimides: Fluorophores for Single Molecule Applications, *Chemistry – An Asian Journal*, **4**, 1542-1550 (2009).

Table of Content:
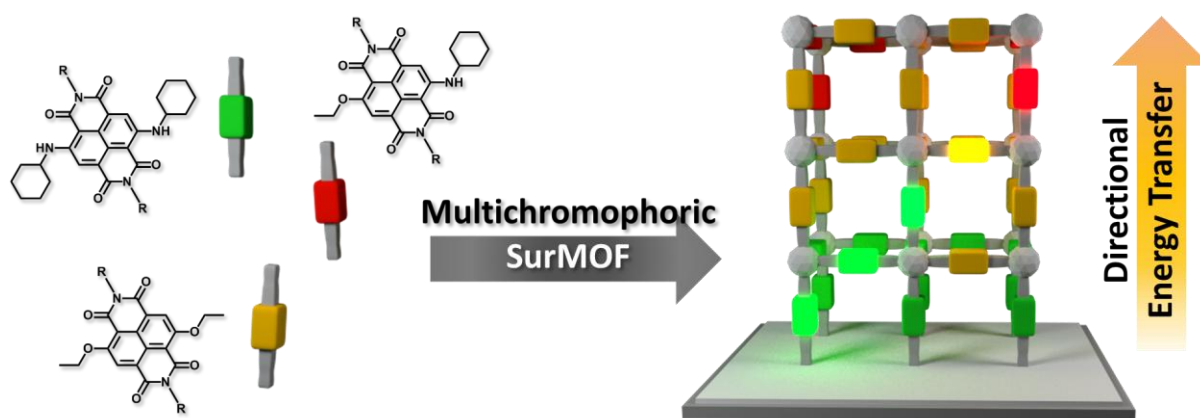
Using an antenna doping strategy in a heterolayer surface-anchored metal-organic framework, directional energy cascade has been realized to convert absorbed blue light to red light with high quantum efficiency.